Boundary-Layer Meteorology (2019) 172:107–132
https://doi.org/10.1007/s10546-019-00440-9

RESEARCH ARTICLE

Testing Various Morphometric Methods for Determining the Vertical Profile of Wind Speed Above Krakow, Poland

Jolanta Godłowska[1] · **Wiesław Kaszowski**[1]

Received: 4 April 2018 / Accepted: 26 February 2019 / Published online: 19 March 2019

Abstract
Various morphometric methods used for wind-speed determination in urban areas inside the roughness sublayer have been tested in Krakow, Poland, using a hybrid modelling system. The hybrid modelling system combines the classic numerical meteorological modelling using ALADIN, MM5, and CALMET models with empirical, non-logarithmic relations determined on the basis of a wind-tunnel experiment. In the hybrid modelling system, the horizontally-averaged wind speed is determined using the displacement height d, roughness length z_0, and an attenuation coefficient α. These parameters are determined using laser scanning data obtained in the MONIT-AIR project. The variability of the selected morphometric parameters in Krakow, the role of the size of the area from which they are determined and the consequences of replacing the frontal area index by the plan area index are analyzed. The different methods used to determine d, z_0, and α are compared and the correctness of the procedures describing the wind profile are verified by comparisons with wind-speed data from road stations, with the wind speed measured between the traffic lanes or at the roadside at a height of 4 m, at standard meteorological stations, and from masts situated on buildings. It is shown that the use of a parametrization based on large-eddy simulations prepared for explicitly resolved buildings in Tokyo and Nagoya in Japan, and taking the maximum instead of the average height of building in empirical relations, significantly improves the modelling results, especially above the average height of buildings.

Keywords Aerodynamic parametrization · Displacement height · Morphometric parameters · Roughness sublayer · Urban wind modelling

1 Introduction

The low-level wind speed is an important factor affecting the quality of life in cities, being a dominant influence on air quality, and one of the key input parameters in air-quality models. The city of Krakow in Poland has long experienced numerous exceedances of pollutant

✉ Jolanta Godłowska
jolanta.godlowska@imgw.pl

[1] Institute of Meteorology and Water Management National Research Institute, 01-673 Warsaw, Poland

concentration standards. This state of affairs is the result not only of large emissions of air pollutants, but also of the unfavourable location of the city that produces a significant reduction in wind speed and, as a consequence, hinders the exchange of air between the city and its surroundings. Recently, in Krakow, large efforts have been made to reduce the emission of air pollutants from heating systems, however, problems can be caused by the constantly increasing emissions from road transport. Thus, there is a need to continuously improve the methods of forecasting air quality in Krakow, in particular relating to smog episodes.

Currently, the air quality forecasting in Krakow is implemented using the Forecasting Air Pollution Propagation System FAPPS [www.smog.imgw.pl], consisting of the meteorological ALADIN, MM5 (PSU/NCAR 2005) and CALMET (Scire et al. 2000a) models, as well as the CALPUFF puff-dispersion model (Scire et al. 2000b). Advances in the field of laser scanning and the improvement of geographic information systems provide the possibility of a better consideration of the urban fabric in meteorological modelling, and thus the potential improvement of air-quality forecasts. This goal was served by the MONIT-AIR project (Bajorek-Zydroń and Wężyk 2016), in which the Krakow morphometric databases, such as the modelling database 'Baza Danych Modelowania' (BDM) and the representative database 'Baza Danych Reprezentatywnych' (BDR), were created on the basis of laser scanning data.

The determination of the wind field in urban areas is hampered because the simulation and parametrization of airflow in cities is extremely difficult. Because of the heterogeneity and the presence of numerous and diverse roughness elements, wind-speed and turbulence profiles in the urban boundary layer (UBL) cannot be properly described using standard Monin–Obukhov similarity theory (MOST) (Stull 1988). Inside the roughness sublayer (RSL), especially in the urban canopy layer (UCL), flow is characterized by high spatial and temporal variability. This variability is forced by buildings and other rigid elements that are irregularly spaced and vary in shape and height, as well as by urban greenery. Only above the RSL, where the direct influence of surface roughness elements can be neglected, is the wind field more homogenous and the wind-speed profile for neutral conditions can be described by the logarithmic relation (Tennekes 1973), incorporating the friction velocity u_*, the roughness length z_0, and the displacement height d.

In our study, different morphometric methods for obtaining d and z_0 have been tested, most having been compared in Grimmond and Oke (1999). Selected morphometric data for Krakow were subjected to detailed analysis, and the scope of their variability in the city area, the possibility of substituting specific parameters by others, and the impact of the size of the area from which their values are determined have been tested.

Because of the fact that different effects play a key role at different scales, it is necessary in cities to adjust the description of the wind field to the adopted scale. Britter and Hanna (2003) suggest four conceptual ranges of length scales in the urban context: regional (up to 100 or 200 km), city scale (up to 10 or 20 km), neighbourhood scale (up to 1 or 2 km), and street-canyon scale (less than 100 m). Numerical weather prediction and air pollution models cannot yet resolve the street-canyon scale, but may attain neighbourhood scale. Unfortunately, in such models MOST theory, even though inappropriate, is still used for wind-field determination within the UBL. However, recently, the urban surface exchange parametrization scheme of Martilli et al. (2002) has been implemented in the Weather Research and Forecasting/Chemistry (WRF/Chem) model as a multilayer urban canopy parametrization (Liao et al. 2014). Due to the extremely diversified and turbulent structure of the airflow in the urban environment, especially when modelling air quality, the wind-speed profile should be described using semi-empirical relations. It is necessary that such

relations should take into account both the results of urban field experiments, as well as the results determined on the basis of wind-tunnel experiments or large-eddy simulation (LES).

For our study the hybrid modelling system has been used to determine wind speed in the RSL in urban areas by using morphometrically-determined parameters d and z_0. The hybrid modelling system is based on the numerical weather prediction system ALADIN/MM5, modified by the CALMET model calculated with a 100-m horizontal grid spacing (the area of a single grid cell is 0.01 km^2) for precisely taking into account urban and terrain effects. The physical properties of each grid mesh have been directly entered from the BDM database, as opposed to the use of land-use classes. The method for obtaining the wind speed inside the UCL is to extrapolate the wind speed from the second layer of the CALMET model with a height of 50 m to within the RSL using relations based on Macdonald (2000) and on the results of LES modelling (Kanda et al. 2013).

The determination of the variability of the wind field in cities is a big challenge as evidenced by the results of numerous urban experiments (Rotach 1995; Grimmond et al. 2004; Rotach et al. 2005; Christen 2005; Mestayer et al. 2005; Britter 2005; Dobre et al. 2005; Hanna et al. 2007, 2009; Barlow et al. 2009). The results of these experiments show that the measured wind speed inside cities is influenced by the height of the anemometer and the distribution of roughness elements around the measurement site. Recently, much information on roughness parameters in cities has been obtained through the analysis of wind-speed measurements at three sites (within 60 m of each other) in London, UK (Kent et al. 2017a, 2018a). The results indicate that morphometric methods used to determine z_0 and d that incorporate roughness-element height variability agree better with anemometric methods (Kent et al. 2017a). Similar conclusions have been attained from the analysis carried out during strong winds (Kent et al. 2018a). The above-mentioned results agree with LES modelling (Kanda et al. 2013) that the wind profile is better determined if the maximum height of buildings and the standard deviation of their height are taken into account when determining z_0 and d from city morphometry. A detailed description of the behaviour of airflow inside the RSL can be obtained from wind-tunnel experiments (Kastner-Klein et al. 2001; Macdonald et al. 1998; Macdonald 2000), which serve to determine the wind profile within the UCL.

For ideal flow within the canopy layer, Cionco (1972) proposed, on the basis of the simple Prandtl mixing-length model, an exponential variation of wind speed given by

$$u(z) = u(H) \exp\left[\alpha\left(z/H_{\mathrm{av}} - 1\right)\right], \tag{1}$$

where $u(H)$ is the horizontal wind speed at the canopy height H, H_{av} is the average height of the roughness elements and α is the attenuation coefficient. Equation 1 has been tested using wind-tunnel data collected for vegetative canopies and arrangements of plastic, wood and wicker elements (Cionco 1972). Similar behaviour of the wind speed was observed for natural and artificial elements, and the value of the attenuation coefficient was seen to increase when the density and flexibility of the roughness elements increase.

Macdonald (2000) tested Eq. 1 and developed a method for determining wind speeds within the UCL. For this purpose, he used wind-tunnel experimental data (Dispersion Modelling Wind Tunnel at the Building Research Establishment – BRE), see Macdonald et al. (1998). In the BRE wind tunnel, the wind speed was measured within uniformly-distributed rigid cubic blocks in two configurations: perpendicular and slanted to the direction of the flow. By fitting the experimental data into Eq. 1, Macdonald (2000) determined a relationship between the attenuation coefficient α and a key urban morphometric parameter, the frontal area index λ_f (defined as, e.g., in Grimmond and Oke 1999). For $\lambda_f < 0.3$ he

obtained an approximate relationship $\alpha \approx k\lambda_f$, with $k = 9.6$. Later, Sykes et al. (2007), based on data from the BRE campaign, determined a dependency of α on λ_f as $\alpha = 10.8\lambda_f$. Hanna (2012), on the basis of the analyses of turbulence observations in cities, suggested that the relation $\alpha = 10.8\lambda_f$ underpredicts the wind speed and turbulence intensity in the lower part of the UCL and that an improved relationship is $\alpha \approx 5\lambda_p$, where λ_p is the plan area index. In the present study the Sykes and Hanna relationships have been used for testing the Macdonald relations.

The novelty of Macdonald's work (Macdonald 2000) was to replace the logarithmic profile inside the RSL and derive separate relations for the wind-speed profile above and below the average height of buildings. In Krakow, thanks to the results of the MONIT-AIR project, the morphometric parameters such as H_{av}, λ_f or λ_p are available and Macdonald's method for determining the wind profile in the RSL are used in the hybrid modelling system as its deterministic part.

It should be noted that in the BRE campaign, all roughness elements were of the same height. Thus, the average height of buildings, taken as the UCL height, was equal to the maximum building height. For this reason, until recently, it was assumed that the average height of the buildings H_{av} can be assumed as a suitable scaling parameter for determining the displacement height d. Recently, Kanda et al. (2013) and Kent et al. (2017a) have shown that, in the case of urban fabric characterized by the presence of buildings of different heights, this approach is insufficient. The LES conducted for explicitly resolved buildings in Tokyo and Nagoya, Japan, (Kanda et al. 2013) show that vertical profiles of the horizontally-averaged momentum flux are influenced not only by the average building height H_{av}, the frontal area index λ_f and the plan area index λ_p, but also by the maximum building height H_{max} and the standard deviation of building height σ_H. The results of these numerical simulations suggested new parametric relations for the determination of d and z_0, taking into account all the above-mentioned parameters. The comparison between the wind-speed profile extrapolation using the logarithmic law and Doppler lidar observations during neutral conditions in London, UK, confirmed that Kanda's method for determining d and z_0 is an improvement to that of Macdonald (Kent et al. 2017a). Herein, an attempt is made to test both of the aforementioned z_0 and d parametrization methods, comparing wind speeds obtained from the hybrid modelling system forecasts with measurements.

Kent et al. (2017b) have shown that vegetation should be included in the morphometric determination of aerodynamic parameters but not in the same way as solid structures. The plan area index and the frontal area index of buildings and trees should be determined separately, and aerodynamic porosity should be used for determining the plan area of vegetation, whereas the frontal area index should be determined assuming a solid structure of the same size. In the hybrid modelling system, the vegetation has been taken into account in this way. Unfortunately, the BDM database does not contain all the morphometric parameters for vegetation needed in the modelling, lacking frontal area indices and standard deviations of tree heights. These parameters have been calculated in an approximate way from the remaining vegetation data available in the BDM database.

2 Methodology

2.1 The Hybrid Modelling System

The hybrid modelling system created for wind-speed determination in Krakow (Fig. 1) combines classic numerical meteorological modelling with empirical Macdonald relations (Macdonald 2000), taking into account the morphometric parameters of the city.

The proper reflection of the synoptic and regional scale effects is ensured by the use of data from the ALADIN model that are an input into the MM5 model (PSU/NCAR 2005). Subsequently, the data from the ALADIN/MM5 model is used in the CALMET model (Scire et al. 2000a, b), which makes it possible to take into account city-scale effects. The computational domain of the CALMET model, which includes the city of Krakow and its surroundings, is presented in Fig. 2.

One of the main factors affecting the wind field in Krakow at the city scale is the terrain, because the city is in the valley of the Vistula River in an area of complex topography. There are hills to the north and south of Krakow that force the airflow along the west–east axis; furthermore, to the west of Krakow, the Vistula Valley is obscured by numerous hills. These play a key role in modifying the wind field in the western part of the city, impeding the flow penetration into the Vistula River valley during the westerly circulation, which is the dominant circulation in Poland. The CALMET model parametrizes terrain effects such as slope flows (Marht 1982), kinematic (Liu and Yocke 1980) and blocking (Allwine and Whiteman 1985) terrain effects. The effects of physical properties of the surface at the city scale were taken into account by applying the following method. Instead of describing through land-use classes, the physical properties of grid cells, such as the albedo, Bowen ratio, the leaf area index (LAI) and anthropogenic heat flux, have been assigned separately for each grid cell using data from the BDM database.

The impact of the neighbourhood scale is incorporated into the hybrid modelling system by using (Macdonald 2000), for $H < z < h_{RSL}$,

$$u(z) = u(H) + \left(u_*/B\right)\ln((A + zB)/(A + HB)), \tag{2a}$$

$$A = l_c - (H/(z - H))\left(\kappa(z - d) - l_c\right), \tag{2b}$$

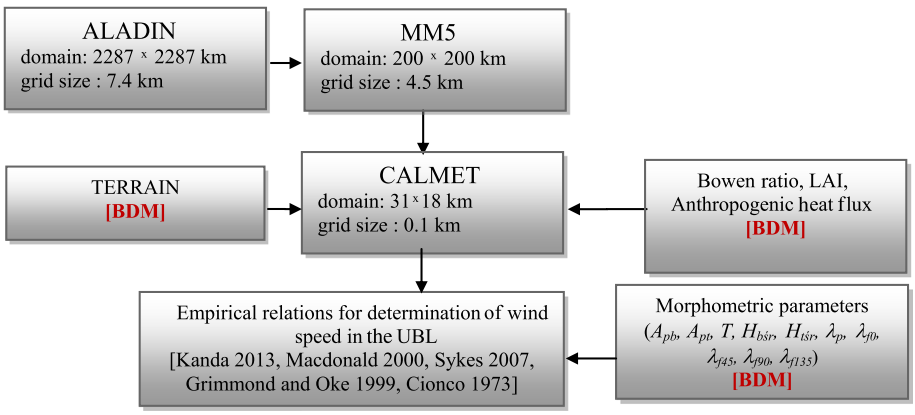

Fig. 1 The hybrid modelling system used for determination of wind speed inside and just above the UCL in Krakow. The BDM abbreviation means that the data have been obtained from the BDM database

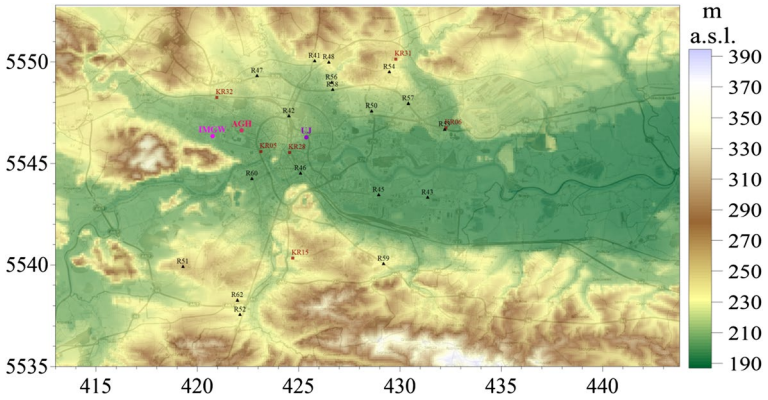

Fig. 2 The physical properties at each grid cell for the CALMET model domain used in the MONIT-AIR project in UTM Zone 34 coordinates. Indicated: the location of air-quality monitoring stations (brown squares), IMGW meteorological station (pink circle), AGH (red) and UJ (violet) meteorological stations, road meteorological station (dark triangles)

$$B = (1/(z-H))\left(\kappa(z-d) - l_c\right), \tag{2c}$$

and for $z < H$,

$$u(z) = u(H)\exp\left[\alpha(z/H - 1)\right], \tag{3}$$

where H is the canopy height, u_* is the friction velocity calculated from the wind speed at 50-m height, l_c is the Prandtl mixing length, $\kappa = 0.4$ is the von Karman constant. It should be noted that the Macdonald approach is only appropriate for neutral conditions. As shown in Fig. 3, the logarithmic wind profile determined for neutral conditions above the RSL has been replaced for flow within the RSL by two different relations defining the wind profile above and within the UCL.

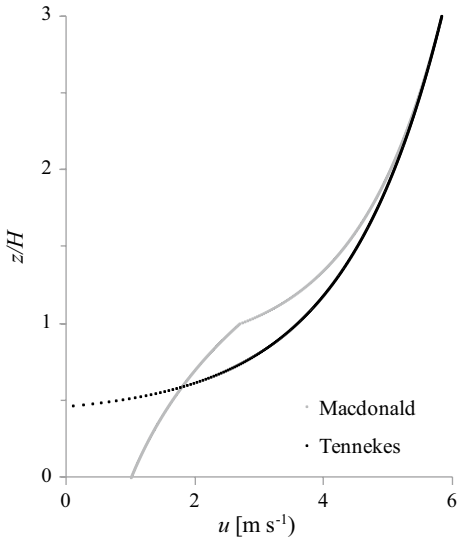

Fig. 3 The comparison of the extrapolated log profile (Tennekes 1973) with the Macdonald profile (example for $\lambda_p = 0.2$, $\lambda_f = 0.12$, $H = 15$ m, $\alpha = 1$, d (Eq. 6), z_0 (Eq. 8), v (50 m) = 6 m s^{-1})

Due to the fact that in Krakow the average height of buildings for the vast majority of grid cells does not exceed 25 m we calculate the wind speed at a height H by using the wind data from the second layer of the CALMET model (50 m). In the CALMET model we have adopted terrain and land-use parameters from the MONIT-AIR project database, but at this stage we do not take into account the roughness of the city. Roughness is incorporated by extrapolating the wind speed from $z = 50$ m using Macdonald's relations firstly down to $z = H$ (2a, 2b, 2c) and then into the UCL (3).

In the first version of the hybrid modelling system, the average height of the roughness elements H_{av} has been taken as the UCL height H. When the Kanda et al. (2013) method for determining z_0 and d is used, the UCL height H is assumed to be the maximum height of the buildings or trees for a given morphometric testing resolution. The presence of trees and shrubs introduces considerable uncertainty into the modelling due to the difficulty in parametrizing the impact of such roughness elements on the wind profile. The size, structure, flexibility, leaf type and age of the vegetation are important in determining the drag coefficient (Gromke et al. 2008; Koizumi et al. 2010; Kent et al. 2017b). Due to the fact that the vast majority of the trees in Krakow are leafy and lose leaves in winter, the winter period is considered to be the most suitable for testing the hybrid modelling system. The plan area index λ_p of both buildings and vegetation in Krakow has been calculated according to the relation

$$\lambda_p = \frac{\sum_{i=1}^{n} A_{pbi} + \beta A_{pt}}{A_T}, \tag{4}$$

where A_{pbi} is the plan area of the building, A_{pt} is the plan area of vegetation in the grid cell, A_T is the total surface area, i refers to each individual building, and β is associated with foliage and varies depending on the season from 0.3 in winter, through 0.4 in spring and autumn to 0.52 in summer. In the MONIT-AIR database there is no frontal area index for vegetation, therefore the frontal area index λ_{ft} for vegetation has been estimated by using

$$\lambda_{ft} = \frac{1.6 h_t \sqrt{A_{pt}/\pi}}{A_T} \tag{5}$$

where h_t is the weighted average height of trees.

2.2 The MONIT-AIR Morphometric Databases (BDM and BDR)

The morphometric data obtained in the MONIT-AIR project (Bajorek-Zydron and Wezyk 2016) makes it possible to take into account the influence of roughness elements on the wind speed inside and just above the UCL. The BDM and BDR morphometric databases were established in the MONIT-AIR project, the aim of which was, inter alia, the integration of spatial-data monitoring for improving air-quality modelling in Krakow. The range of information and the method of determination of morphometric parameters are compatible with the National Urban Data and Access Portal Tool (NUDAPT) (Burian and Ching 2009; Glotfelty et al. 2013). To obtain morphometric data, a variety of data available to the administrative area of the city have been used, including: boundaries and numbers of parcels (EGiB) from the State Geodetic and Cartographic database, airborne laser-scanning data for the city of Krakow in July 2012, high-resolution multispectral satellite imaginary WorldView2 on 9 October 2014, and object-oriented classification (11 classes based on

Rapid Eye satellite images of 21 August 2010 – 5-m resolution). In addition, based on the population density in districts of Krakow and the cubic capacity of buildings, the anthropogenic heat flux was estimated (Xie et al. 2016a, b). The leaf area index, *LAI*, was estimated based on the normalized difference vegetation index (Tian et al. 2017).

The morphometric parameters were calculated twice: firstly for squares of 0.01 km^2, the same as the mesh of the CALMET model domain (Fig. 2) covering the area of a rectangle with sides parallel to the north–south direction (180 grid points) and east–west direction (310 grid points) and entered into the BDM database. In the alternative BDR database, the same morphometric parameters were calculated for 44 relatively large representative areas with typical Krakow types of urban fabric: the historical centre of the city, residential, single-family housing, commercial and industrial areas, urban greenery and forests. The total area of the BDR database is approximately 10% of Krakow's area. Representative areas were chosen so that each of them was relatively homogeneous and typical, and for each type of urban fabric, several representative areas have been selected to examine the variability of morphometric parameters within each class.

The most important morphometric parameters used in the hybrid modelling system are: the average height of buildings/trees weighted by their surfaces (H_{avb} and H_{avt} respectively), the standard deviation of the buildings heights σ_b, total area occupied by buildings/trees and shrubs (A_{pb} and A_{pt} respectively) as well as the plan area density λ_p (z) and the frontal area density λ_f (θ_i, z) for θ_i=0°, 45°, 90°, 135° and z=0, 5, 10, 15 … 70 m (λ_p (0) denoted later as λ_p and λ_f (θ_i, 0) where θ_i=0°, 45°, 90°, 135° denoted later as λ_{f0}, λ_{f45}, λ_{f90}, λ_{f135}). The values of selected morphometric parameters from the BDR database are shown in Appendix 1.

The BDM database allows the determination of the range of parameter variations inside a computational domain. In the hybrid modelling system both buildings and trees are taken into account as roughness elements, and the maximum of the area-weighted average effective height of trees H_{tef} and the area-weighted average height of buildings H_{avb} is the basis for determining the UCL height H in each grid in the hybrid modelling system. The height H_{tef} is chosen to be 80% of the average height of trees H_{avt} (Holland et al. 2008); the values of H_{avb} and H_{avt} are compared in Fig. 4. In the predominant area of the computational domain, especially in the city centre, the height of the buildings is greater than the height of the trees, the exception being the area of the Wolski Forest, Borkowski Forest and old cemeteries. The average height of both buildings and trees for the most grid cells of the

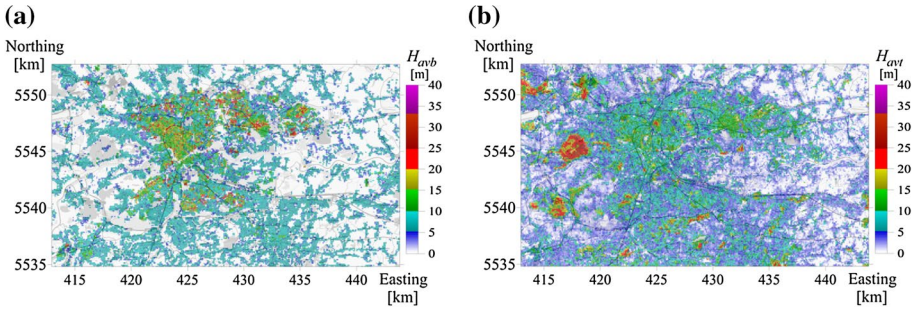

Fig. 4 Area-weighted mean building height H_{avb} (**a**), and area-weighted mean vegetation height H_{avt} (**b**) from the BDM database in UTM Zone 34 coordinates

computational domain does not exceed 25 m; moreover, the H_{avb} field is less homogenous than that of H_{avt}.

Information about the packing density of buildings and trees is used to determine the plan area index $\lambda_{p.}$ Maps of grid area occupied by buildings and vegetation are compared in Fig. 5; for buildings, the packing density for most grids in the computational domain <0.35, indicating that within the domain we are primarily dealing with two flow regimes: "isolated flow" outside the city and weak interference flow within the city. However in the city centre and in some small areas outside the city centre, mainly industrial, the "skimming flow" regime may occur (Hussain and Lee 1980).

2.3 The Morphometric Methods to Determine *d* and z_0

Three different pairs of d and z_0 were tested in the hybrid modelling system.

1. In the first testing scenario, later referred to as the GOM scenario, the plan area index λ_p has been used to determine both d and z_0.

   For determining the displacement height d, the original Macdonald relation (Macdonald et al. 1998) has been used,

$$d(\mathrm{MD})/H_{\mathrm{av}} = 1 + A^{-\lambda_p}\left(\lambda_p - 1\right) \tag{6}$$

   where $A = 4.43$.

   For determining $z_{0,}$ the relations based on Fig. 1 of Grimmond and Oke (1999) were prepared, later referred to as z_0(GO),

$$z_0(\mathrm{GO})/H_{\mathrm{av}} = 0.3\lambda_p, \quad \lambda_p \le 0.35 \tag{7a}$$

$$z_0(\mathrm{GO})/H_{\mathrm{av}} = -0.3\lambda_p + 0.225, \quad 0.35 < \lambda_p < 0.7 \tag{7b}$$

$$z_0(\mathrm{GO})/H_{\mathrm{av}} = 0.015 \quad \lambda_p > 0.7 \tag{7c}$$

2. In the second testing scenario, later referred as the MD scenario, both original Macdonald relations have been used, in which d has been determined using the plan area index $\lambda_{p,}$ while z_0 has been determined using the frontal area index λ_f. The displacement height d in this scenario has been determined using Eq. 6.

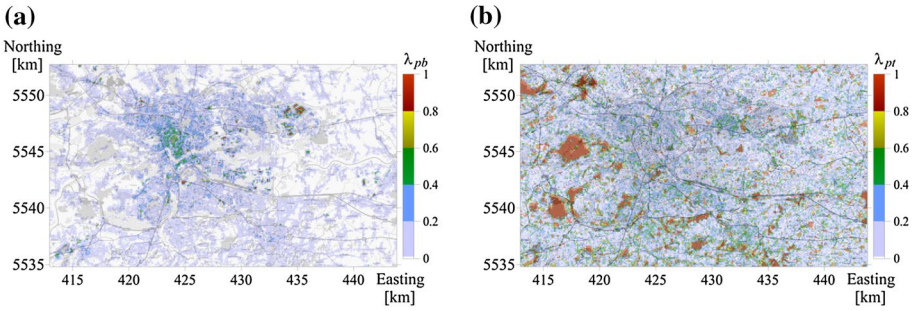

Fig. 5 The plan area index for buildings λ_{pb} (**a**), and vegetation λ_{pt} (**b**) from the BDM database in UTM Zone 34 coordinates

For determining $z_{0,}$ the original Macdonald relation (Macdonald et al. 1998) has been used,

$$z_0(\mathrm{MD})/H_{\mathrm{av}} = \left(1 - d/H_{\mathrm{av}}\right)\exp\left[-\left\{0.5\beta(C_{lb}/\kappa^2)\left(1 - d/H_{\mathrm{av}}\right)\lambda_{\mathrm{f}}\right\}^{-0.5}\right], \tag{8}$$

where $\beta = 1.0$, $C_{lb} = 1.2$ is the drag coefficient of an obstacle.

3. In the third testing scenario, later referred as the KAN scenario (Kanda et al. 2013), the roughness-element height variability has been directly considered through the use of the maximum (H_{max}) and the standard deviation (σ_h) of roughness-element heights and incorporates z_0(MD), such that,

$$d(\mathrm{KAN})/H_{\mathrm{max}} = c_0X^2 + (a_0\lambda_P^{b0} - c_0)X, \tag{9}$$

$$z_0(\mathrm{KAN})/z_0(\mathrm{MD}) = b_1Y^2 + c_1Y + a_1, \tag{10}$$

where $X = (\sigma_h + H_{av})/H_{max}$, $Y = \lambda_p\sigma_h/H_{av}$, $0 \le X \le 1$, $0 \le Y$ and a_0, b_0, c_0, a_1, b_1 and c_1, are constants with values of 1.29, 0.36, 0.17, 0.71, 20.21 and 0.77, respectively.

The wind speed from the hybrid modelling system for the GOM testing scenario was verified only for morphometric parameters obtained for a circle of 200-m radius around the observational site and for $\alpha = 10.8\lambda_f$ (Sykes et al. 2007). The investigation on how the size of the area from which the morphometric information is obtained affects the results of the modelling has been performed only in the MD and KAN testing scenarios. For this purpose, morphometric parameters have been obtained from four square areas of different size with a station in the centre; areas are of size 9, 25, 49 and 81 grid cells with a side of 100 m. In addition, two different options for calculating the attenuation factor α from Eq. 2—both Sykes's $\alpha = 10.8\lambda_f$ and Hanna's $\alpha = 5\lambda_p$ have been tested. Table 1 compares testing scenarios with their references, morphometric parameters required for calculations, areas from which morphometric parameters were determined and methods for determining the α attenuation factor.

2.4 Statistical Measures for Verification of Wind-Speed Predictions from the Hybrid Modelling System

The accuracy of the wind-speed forecasts from the hybrid modelling system was verified using data from 1 January to 31 March 2013 taken from 18 road meteorological stations, one IMGW station with a standard measurement height of 10 m and two masts situated on the roofs of university buildings: measurements at 20-m height (AGH station) and at 22-m height (UJ station). For the road stations, the wind speed is measured between the traffic lanes or at the roadside, at a height of 4 m. For station positions, see Fig. 2, and for the morphometric characteristics of the surroundings of each measurement station, see Appendix 2. Although all stations were provided with data quality control, we independently checked the quality of the measurement series, with particular attention given to the completeness of the data series and the consistency of the data. The consistency was analyzed directly by comparison of the series from different locations. As a result of the data quality control we approved 18 out of 21 data series of road stations, and in this way, we have used 21 wind-speed data series for study.

The location of the measurement station plays a key role in shaping the wind speed. The stations' surroundings characteristics described by the morphometric parameters and

Table 1 Description of different testing scenarios. For each option the references were given to calculate the displacement height d and aerodynamic roughness length z_0. In the last column, the morphometric parameters necessary for the calculation are specified. In the fourth column the area used for determination of morphometric parameters is presented. In the fifth column the methods of calculating the attenuation factor α are shown: (H) for Hanna (2012) and (S) for Sykes et al. (2007), respectively

Scenarios	z_0 [m]	d [m]	Area [km^2]	Attenuation factor α	Morphometric parameters
GOM_13_H	$z_0 = f(H_{av}, \lambda_p)$ Equation 7a Figure 1 (Grimmond and Oke 1999)	$d = f(H_{av}, \lambda_p)$ Equation 6 (Macdonald et al. 1998)	0,13	$5\lambda_p$ H	H_{av} λ_p
GOM_13_S			0,13	$10.8\lambda_f$ S	H_{av} λ_p, λ_f
MD_09_H	$z_0 = f(H_{av}, \lambda_f)$ Equation 8 (Macdonald et al. 1998)	$d = f(H_{av}, \lambda_f)$ Equation 6 (Macdonald et al. 1998)	0.09	$5\lambda_p$ H	H_{av} λ_p, λ_f
MD_16_H			0.16		
MD_25_H			0.25		
MD_81_H			0.81		
MD_09_S			0.09	$10.8\lambda_f$ S	
MD_16_S			0.16		
MD_25_S			0.25		
MD_81_S			0.81		
KAN_09_H	$z_0 = f(H_{av}, \lambda_f, \lambda_p, \sigma_h)$ Equation 10 (Kanda et al. 2013)	$d = f(H_{av}, H_{max}, \lambda_p, \sigma_h)$ Equation 9 (Kanda et al. 2013)	0.09	$5\lambda_p$ H	$H_{av}, H_{max}, \lambda_p, \lambda_f, \sigma_h$
KAN_16_H			0.16		
KAN_25_H			0.25		
KAN_81_H			0.81		
KAN_09_S			0.09	$10.8\lambda_f$ S	
KAN_16_S			0.16		
KAN_25_S			0.25		
KAN_81_S			0.81		

classified using a new local climate zone (LCZ) classification system (Stewart and Oke 2012; Stewart et al. 2014) are shown in Appendix 2. For verification of wind-speed prediction from the hybrid modelling system we have compared the average values of measurements u_O and model results u_P and the standard deviation of measurements σ_O and model results σ_P, respectively. Moreover, we have calculated (Schlunzen and Sokhi 2008)

– the average difference bias,

$$BIAS = \frac{1}{N}\sum_{i=1}^{N}(u_{\mathrm{P}i} - u_{\mathrm{O}i}) \tag{11}$$

– the root-mean-square error,

$$RMSE = \sqrt{\frac{1}{N}\sum_{i=1}^{N}\left(u_{\mathrm{P}i} - u_{\mathrm{O}i}\right)^2} \tag{12}$$

– the correlation coefficient,

$$r = \sum_{i=1}^{N}\left(u_{\mathrm{O}i} - u_{\mathrm{O}}\right)\left(u_{\mathrm{P}i} - u_{\mathrm{P}}\right)/N\sigma_{\mathrm{O}}\sigma_{\mathrm{P}} \tag{13}$$

– the hit rate

$$HR = \frac{1}{N}\sum_{i=1}^{N}\left(n_i\right) \text{ with } n_i = \begin{cases} 1 & \text{for } |u_{\mathrm{P}i} - u_{\mathrm{O}i}| \le 1\ \mathrm{m\,s^{-1}} \\ 0 & \text{else} \end{cases} \tag{14}$$

where N is the number of data points, $u_{\mathrm{P}i}$ and $u_{\mathrm{O}i}$ are the modelled and measured wind speed at time i, u_{P} and u_{O} are the average values of model results and measurements, respectively.

3 Results

3.1 The Relationship Between the Frontal Area Index λ_f and the Plan Area Index λ_p in a Real City using the Example of Krakow

The frontal area index data λ_f as well as the plan area index data λ_p are crucial for determining the displacement height d, the roughness length z_0, and the attenuation coefficient α that control the wind profile within the UCL. The data collected in the BDM database provide knowledge of the dependence of λ_f with the wind direction over Krakow. In order to study the differences between λ_{f0}, λ_{f45}, λ_{f90} and λ_{f135}, for the whole city, the mean, standard deviation and selected percentiles have been calculated (Table 2).

In addition, taking λ_{f0} as a base, the comparative characteristics such as *RMSE* and the correlation coefficient r for λ_f pairs were also calculated. One can see that there are slightly more buildings in Krakow located parallel to the Vistula Valley, although the observed inhomogeneity is small. Table 2 allows us to compare λ_p with λ_f, noting that the average λ_p value is about twice that of λ_f, but for a median $\lambda_p \approx 4\lambda_f$ or $\lambda_p \approx 6\lambda_f$. The results presented in

Table 2 The comparative characteristics of the frontal area indices for the four wind-direction sectors N (λ_{f0}), NE (λ_{f45}), E(λ_{f90}) and SE(λ_{f135}) and the plan area index(λ_p) calculated for resolution 0.01 km^2

	Resolution [km^2]	Average value	Median	75th percentile	90th percentile	Max	Standard deviation	*RMSE* (λ_{f0})	*r* (λ_{f0})
λ_p	0.01	0.071	0.012	0.110	0.214	1.000	0.112	0.086	0.761
λ_{f0}	0.01	0.033	0.002	0.044	0.101	0.675	0.060	0.000	1.000
λ_{f45}	0.01	0.037	0.003	0.049	0.113	0.770	0.066	0.018	0.965
λ_{f90}	0.01	0.032	0.002	0.042	0.098	0.885	0.059	0.025	0.908
λ_{f135}	0.01	0.037	0.003	0.048	0.112	0.831	0.065	0.019	0.959

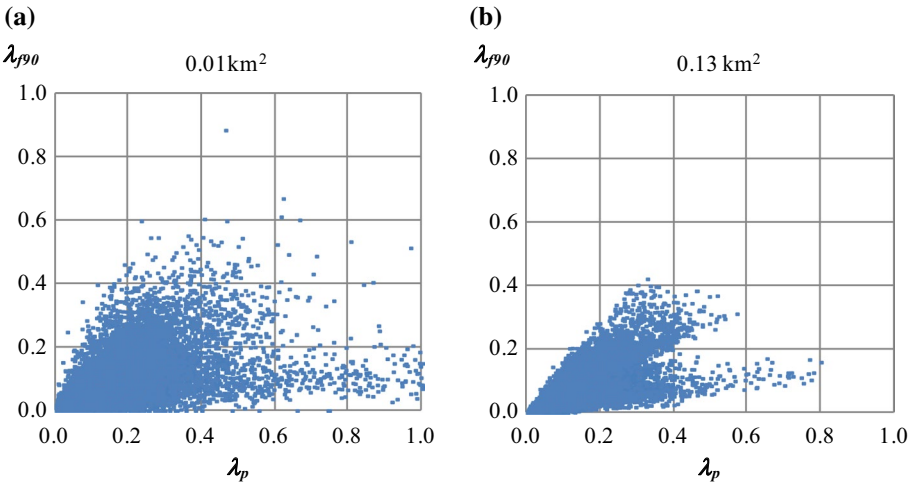

Fig. 6 The comparison between the plan area index λ_p and the frontal area index λ_{f90} shown for original data (morphometric information from 0.01 km^2—**a**) and spatially-averaged data (morphometric information from about 0.13 km^2—**b**)

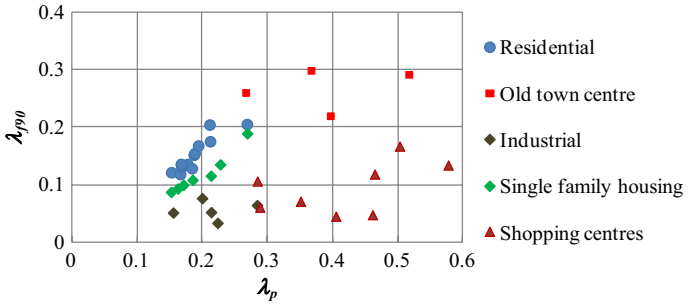

Fig. 7 The comparison between the plan area index λ_p and the frontal area index λ_{f90} calculated for different types of urban fabric: the historical centre of the city, residential, single-family housing, shopping centres and industrial areas

Table 2 show a non-linear relationship between λ_f and λ_p and suggest a large spread of data, and may be due to determining λ_f and λ_p from small areas that are too small. The results obtained for morphometric information calculated for an area of 0.01 km^2 and data averaged over a 200-m radius (about 0.13 km^2) show a large spread for both datasets (Fig. 6).

The large scatter observed in Fig. 6a, b partly corresponds to the results from the BDR database presented in Fig. 7. Comparing λ_p with λ_f calculated for representative areas from the BDR database shows that for housing estates and single-family housing, one notes the similarity between λ_f and λ_p, while for shopping centres and industrial areas regardless of the value of λ_p, the value of $\lambda_f < 0.1$. Exceptions ($0.1 < \lambda_f < 0.2$) are shopping centres located in areas with $\sigma_b \geq 2.5$ m and $H_{avb} > 10$ m. In Krakow, these areas are classified using local climate zone (LCZ) classes (Steward and Oke 2012) as LCZ = 2, LCZ = 8_1 or LCZ = 8_5 (see Appendix 1).

3.2 The Comparison of Various Morphometric Methods for Determining *d* and z_0

Currently, for many cities there is a lack of frontal area index data. Moreover, in areas with complex topography λ_f cannot be used in modelling because of the inability to correctly identify the wind direction. The lack of the λ_f data enforces the use of λ_p instead of λ_f. Grimmond and Oke (1999) suggested computing d and z_0 based on Bottema (1995), Raupach (1994, 1995) and Macdonald et al. (1998). Here, the Hanna (2012) relations are also taken into consideration, and of these four relations, only the Macdonald relation (Macdonald et al. 1998) makes it possible to use λ_p for the calculation of d. Figure 8 compares the d/H values obtained using all mentioned relations, and shows that the discrepancy between the different estimates of d is not mainly due to the choice of the morphometric parameter (λ_p or λ_f). A good correspondence between Macdonald's method (Macdonald et al. 1998) and Bottema's method (1995) suggests that, in the absence of λ_f data, the determination of d by Macdonald's method using λ_p is a good alternative.

Figure 9a, b compares the z_0/H values obtained using the Raupach (1994), Macdonald et al. (1998), Hanna (2012) and GO methods (Eq. 7a–7c). The GO method of computing z_0/H using λ_p gives a reasonable value of z_0. In addition, a comparison of different methods using λ_f does not clearly show a better correspondence than the comparison of these methods using the GO method.

After careful analysis we have chosen for testing two pairs of d and z_0 determination methods for the average roughness-element height H_{av} taken as the canopy height H. In the GOM scenario, the hybrid modelling system uses Macdonald's relation to calculate the displacement height d and the GO relations (Eq. 7a–7c) for the calculation of roughness length z_0. In the MD scenario both parameters d and z_0 are obtained using Macdonald's relations.

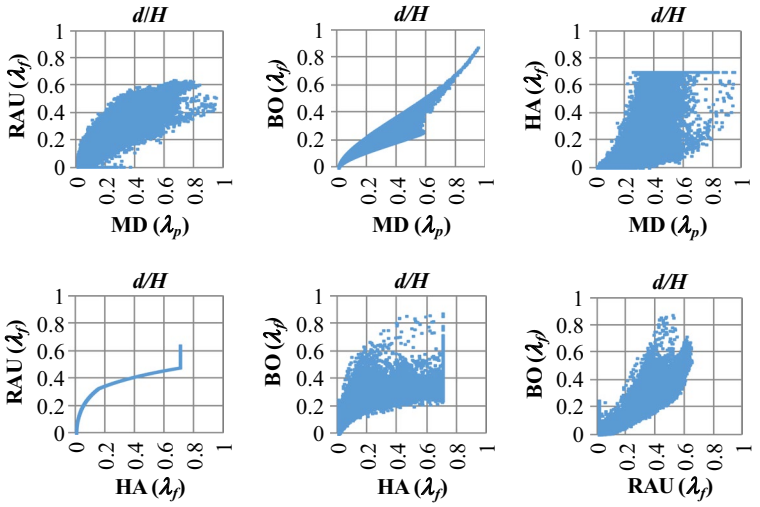

Fig. 8 The comparison between the displacement height d with respect to mean element height H calculated using different morphometric methods. Morphometric-method abbreviations: MD(λ_p) Macdonald et al. (1998), BO(λ_f) Bottema (1995), HA(λ_f) Hanna (2012) and RAU(λ_f) Raupach (1994)

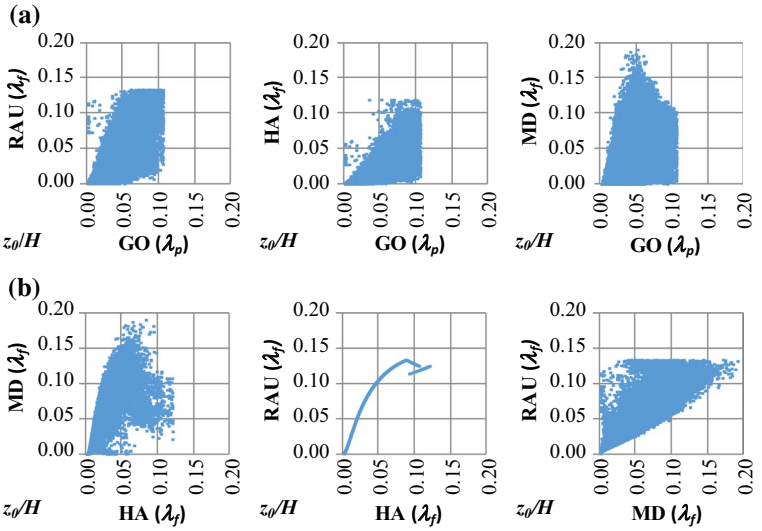

Fig. 9 The comparison between roughness length z_0 with respect to mean element height H calculated using MD(λ_f) (Macdonald et al. 1998), HA(λ_f) (Hanna 2012) and RAU(λ_f) (Raupach 1994, 1995) methods taking into account frontal area fraction λ_{f45} (**b**) and between these methods and the GO method (Eqs. 7a–7c) taking into account the plan area index λ_p (**a**)

3.3 Wind-Profile Modelling in the Roughness Sublayer

Road stations are located in different local climate zones of the city and roughness elements in their environment form a canopy layer of different heights. Therefore, despite the same height of 4 m at which the wind speed is measured, these measurements, due to the differences in the UCL height, allow us to verify the correctness of determining the wind profile inside the UCL. The average hourly wind speeds for the first three months of 2013 have been analyzed, and for the GOM_13_S scenario the verification of wind-speed forecasts was carried out separately for all data and for moderate to high wind speeds only ($v \geq 3$ m s^{-1} measured at 10 m at the synoptic station at Krakow Balice airport, located west of the city).

A clear dependence of *BIAS* values on λ_p and z/H_{avb} has been observed for both sets of data, as shown in Fig. 10a, b. A similar behaviour for all data and the subsample of high wind speeds (about 67% of the sample) indicates that the observed effect is not related to atmospheric stability. The *BIAS* dependence on λ_p in Fig. 10a, b has been presented only for road stations, since measurements carried out above H_{avb} do not show such a relationship. A high positive *BIAS* value is observed mainly for stations located at a height greater than the average building height H_{avb}, as shown in Fig. 10c, d. The detailed analysis shows that the removal of the above-mentioned clear systematic effects is not possible without changing the method of determining H in Eqs. 2 and 3.

The comparison of *BIAS* values calculated for the MD_81_S and KAN_81_S scenarios shown in Fig. 11a, b demonstrates that accepting the H value as the maximum height H_{max} of the roughness elements and considering H_{max} and σ_h of the roughness elements in determining d and z_0 in the KAN_81_S scenario significantly improves the modelling results, especially in the case of measurements above the average height of buildings. This conclusion is further supported by a direct comparison of the measured and forecast average wind speeds for both options as shown in Fig. 12a, b. Figure 11 shows a significant reduction in

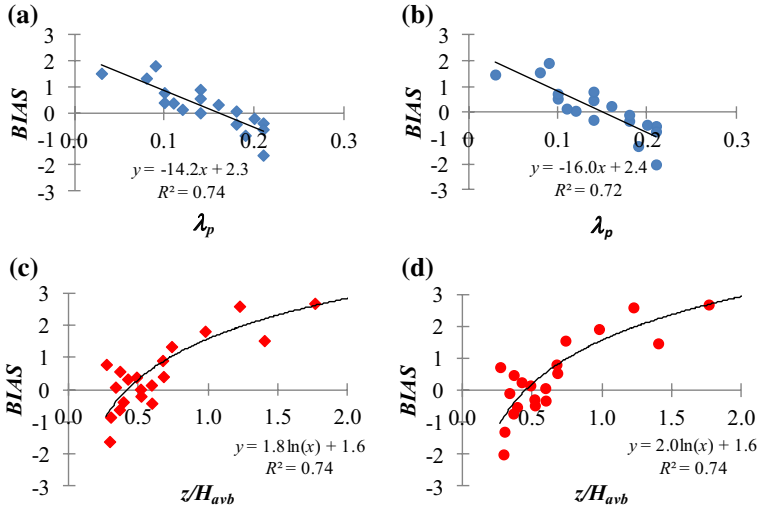

Fig. 10 The relationship between *BIAS* values [m s^{-1}] calculated for the GOM_13_S scenario and the plan area index λ_p (a and b, only for road stations) as well as the measurement height normalized by average building height H_{avb} (c and d) for all data (**a**, **c**) and for wind speed ≥ 3 m s^{-1} at 10-m height at the Krakow Balice synoptic station (**b**, **d**). The sample size: 2160 h, January, February and March 2013

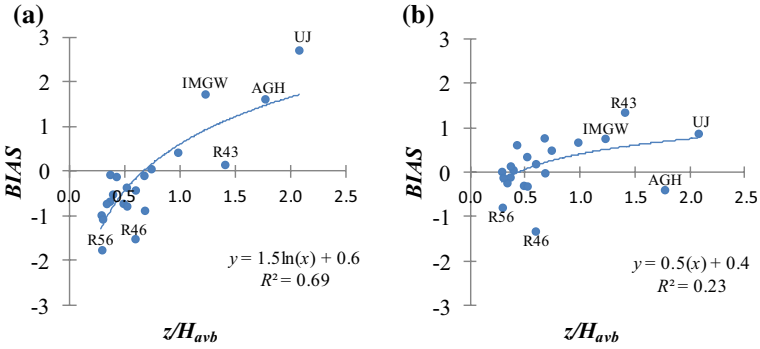

Fig. 11 The relationship between *BIAS* [m s^{-1}] and wind-speed measurement height z, normalized by average building height H_{avb} for the MD_81_S (**a**) and KAN_81_S (**b**) scenarios. Stations with large *BIAS* values have been marked (for identification see Appendix 1 and 2 and Fig. 2). The sample size as in Fig. 10

the forecast wind speeds as compared to the observations at R46 and R56 stations for both scenarios, as well as an overestimation of forecasts at the R43 station for the KAN_81_S scenario (see Fig. 2 and Appendix 2 for station identification). Station R46 is the only station located on the Vistula riverbank. In this case the underestimation of forecast may be the result of flow acceleration in the open corridor formed by the basin in which the Vistula river flows, emphasized by embankments and by dense buildings near the river. In the case of station R56 there is no clear explanation for this behaviour, but may be due to the location of the station on a large roundabout with high buildings and shelters along the roads. Another reason may be the atypical nature of high-rise buildings that contain oversized bunk parking lots. The overprediction of forecast wind speed compared to the R43 station

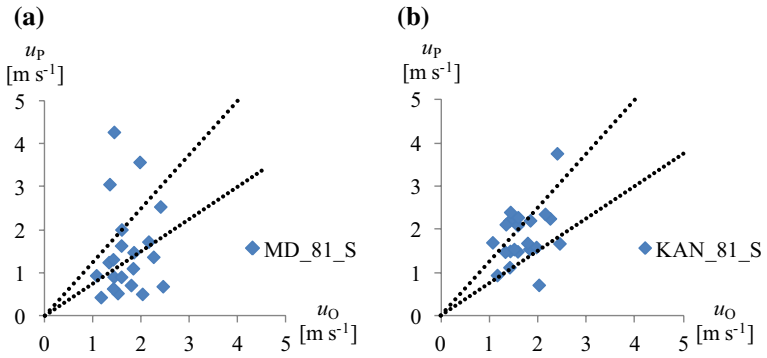

Fig. 12 The relationship between observed u_O and predicted u_P mean wind speed calculated for the period 1 January 2013–31 March 2013 obtained for the MD_81_S (**a**) and KAN_81_S (**b**) scenarios. The sample size as in Fig. 10. The dotted lines indicate the area with the predicted mean wind-speed error less than 25% of the observed mean wind speed

observation may be the result of the sparse arrangement of small buildings around it. In this case, the MD scenario gives much improved results.

The KAN relations (Kanda et al. 2013) for determining d and z_0 were obtained for Nagoya, Japan based on morphometric parameters determined for an area of 1 km^2. Using data from Krakow, we have checked how the size of the area affects the morphometric parameters used in modelling the wind profile (see Fig. 13). The comparison of modelling results for the KAN_9_S, KAN_25_S, KAN_49_S and KAN_81_S scenarios indicates a general correspondence of the obtained results only for areas of 0.25, 0.49 and 0.81 km^2. For several stations the results obtained for the morphometric parameters determined for the area of 0.09 km^2 are clearly different (Fig. 13). These are mainly the stations with the main class LCZ = 4, i.e. with a loose arrangement of tall buildings (R47, R48, R54, R56, AGH), or stations located close to the border of two distinctly different LCZ classes (R42 and R46). The location of the stations is shown in Fig. 2. How this arrangement of urban space is reflected in the morphometric parameters can be seen in Appendix 2.

The comparison of the results obtained for the KAN_S and KAN_H scenarios shows that the two different methods used to obtain the attenuation factor α using λ_f and λ_p in a real city such as Krakow can be used interchangeably. The biggest differences were

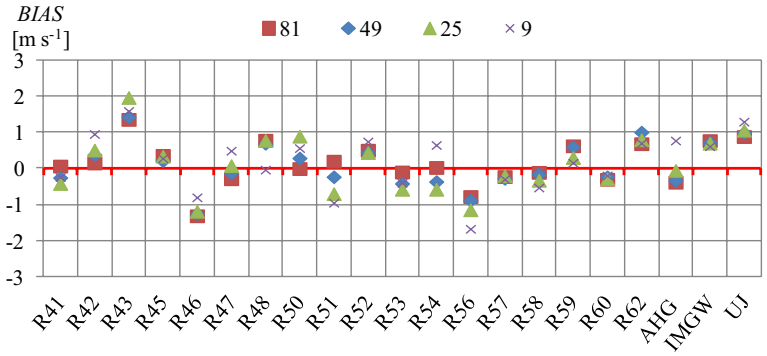

Fig. 13 The comparison of *BIAS* values in mean wind speed [m s^{-1}] calculated for the KAN option for four sizes of areas included in the determination of morphometric parameters—0.09, 0.25, 0.49 and 0.81 km^2

observed in the case of the R43 station with low cubic buildings and the R54 station, with a huge hospital building nearby. The location of both stations is an extreme case of homogeneity (R43) and inhomogeneity (R54) of the building height.

4 Conclusions

The morphometric database for the city of Krakow created within the MONIT-AIR project was used to test various parametric relations describing the mean wind speed inside and just above the urban canopy layer. For this purpose, a hybrid modelling system has been used, which combines classic numerical meteorological modelling using ALADIN, MM5 and CALMET models with empirical relations (Macdonald 2000) based on Cionco (1972). The parameters controlling the wind profile in the roughness sublayer such as urban canopy height H, the displacement height d and roughness length z_0 have been determined using different morphometric methods such as those of Kanda (2013), Macdonald et al. (1998), Bottema (1995), Raupach (1994, 1995). Moreover, the Hanna (2012) and Sykes et al. (2007) relations have been used for the determination of the attenuation coefficient α. In all mentioned relations the knowledge of the plan area index λ_p or the frontal area index λ_f is required. These parameters have been obtained for areas of 0.01 km^2, 0.09 km^2, 0.13 km^2, 0.25 km^2, 0.49 km^2, 0.81 km^2. The tests carried out showed that the surface area over which the roughness parameters are determined should be at least 0.25 km^2 and the best results have been obtained for 0.81 km^2. It follows that the recommended surface from which morphometric parameters should be determined is an area of about 1 km^2.

The analysis of morphometric parameters for Krakow shows that the λ_p value is on average about twice λ_f. However, despite the finding of such general regularity, significant differences in the ratio λ_p to λ_f for different types of urban areas fabric have been observed. For housing estates, residential and single-family housing one can notice similar values of λ_f and λ_p, while for industrial areas and shopping centres located outside the city centre $\lambda_f<0.1$, regardless of the value of λ_p. Summing up, the replacement of λ_p and λ_f in cities with heterogeneous urban fabric is acceptable and for most areas $\lambda_p \approx 2\lambda_f$ can be accepted; however, for cities with large areas with homogeneous urban fabric another estimation should be used that distinguishes shopping centres outside city centre and industrial areas, where it would be more appropriate to adopt $\lambda_f \approx 0.1$ and for residential areas where it would be more appropriate to adopt $\lambda_p \approx \lambda_f$. This result also suggests that for cities with a heterogeneous urban fabric, the Sykes (Sykes et al. 2007) relation $\alpha = 10.8\lambda_f$ gives similar values of the attenuation factor α as for the Hanna (2012) relation $\alpha = 5\lambda_p$. Similar dependencies should be expected for other European cities similar in size and type of development to Krakow. The comparison of morphometric parameters within the same types of urban fabric for different and the same types of local climate zone shown in Appendix 1 may allow assesment of the ratio of λ_p to λ_f for other cities, except for cities with the occurrence of compact high-rise class LCZ1 (Stewart and Oke 2012).

The first three months of 2013 taken for testing are typical of winter in Poland with average monthly temperatures below 0 °C. The frost wave in the third decade of March inhibited vegetation growth, and therefore, it can be assumed that in terms of vegetation, the data are uniform. On the other hand, this period was characterized by a large enough circulation variability, hence it appears to be sufficient for testing. The tests were carried out only for the period close to the date of laser scanning, so that the fast-moving urbanization processes in recent years have not introduced additional uncertainty for modelling.

Based on the comparison of mean wind-speed statistics at the hybrid modelling system that used the Macdonald (2000) relations (2a–2c) and (3) and from observational datasets at

21 sites having z/H_{av} from 0.25 to 2.1 it is found that the Kanda et al. (2013) relations (9) and (10) for determining d and z_0 using the maximum height of obstacles H_{max} in combination with its standard deviation, σ_H are appropriate. Typically, the errors (*BIAS*, *RMSE*) with these choices are −0.4 to 1 m s^{-1} (*BIAS*) and 1–1.5 m s^{-1} (*RMSE*) for wind-speed estimation above z/H_{av}=0.8 and −0.3 to 0.8 m s^{-1} (*BIAS*) and 0.8–1.4 m s^{-1} (*RMSE*) for street level estimates. Larger errors appear when wind measurements are made at the border of areas with significantly different LCZ classes (Stewart and Oke 2012). Our results are consistent with the results of a comparison of nine different methods for determining d and z_0 in London, UK (Kent et al. 2017a), whose conclusion is that morphometric methods that incorporate roughness-element height variability agree better with anemometric methods.

In most cities, the impact of vegetation should be taken into consideration, but not in the same way as solid structures (Kent et al. 2017b). Numerous studies indicate that the drag coefficient for vegetation varies with wind speed, with higher drag at lower wind speeds (Mayhead 1973; Rudnicki et al. 2004; Vollsinger et al. 2005; Koizumi et al. 2010). It seems extremely difficult in modelling to properly take into account all parameters influencing the drag due to vegetation. For example, the MONIT-AIR morphometric database does not include the maximum and standard deviation of tree heights. Currently, due to the lack of parameters determining the manner of vegetation distribution and lack of knowledge on the relationship of such parameters with the drag inserted by vegetation, it is inevitable that errors in modelling the average wind speed for foliage periods will be larger, but it is difficult to assess how much. That is why the winter period was considered the most suitable for evaluation of urban local-scale aerodynamic parameters used for the determination of the vertical profile of wind speed in urban areas.

The conducted research has shown that the morphometric parameter database for modelling the wind profile in cities should include statistical characteristics such as the mean, standard deviation and maximum height not only for buildings but also for vegetation, in order to properly use the Kanda et al. (2013) relations. The calculation of λ_f and λ_p for vegetation is a big challenge due to the shape of the crown of trees, the porosity depending on the season and distribution of vegetation, although recent studies (Kent et al. 2017b, 2018b) have made significant progress in this area. Moreover, additional parameters describing how vegetation is distributed, whether it is dispersed or concentrated inside the grid cell, should be introduced. For these reasons, for modelling of the wind field one should rather use the morphometric databases created using laser-scanning data.

Acknowledgements We would like to thank anonymous referees for all valuable comments and suggestions that allowed to greatly improve the exposition of the manuscript. We are grateful for the provision of wind data to the Department of Climatology of the Jagiellonian University in Krakow and the Faculty of Physics and Computer Science of AGH University of Science and Technology (Krakow) as well as to the City of Krakow Office for sharing data from the TRAX road stations. This research was financially supported by Financial Mechanism of the European Economic Area 2009–2014 in the project MONIT-AIR entitled "Integrated monitoring system of spatial data to improve air quality in Krakow".

Appendix 1

See Table 3

Table 3 Selected morphometric features of representative areas in the BDR database. Building and land-cover types are determined based on local climate zones LCZ (Stewart and Oke 2012; Stewart et al. 2014). The variables H_{avb} and H_{avt} are the average heights of buildings and trees, weighted by their surfaces, respectively; σ_b is the standard deviation of the buildings heights; λ_{pb} and λ_{pv} are the plan area indices for buildings and vegetation, respectively; λ_{fb} is the frontal area index for buildings calculated for four sectors 0°, 45°, 90°, 135°

Class	LCZ class	Area [km^2]	$H_{avb.}$ [m]	σ_b [m]	$H_{avt.}$ [m]	λ_{pb}	λ_{fb}				λ_{pv}
							0°	45°	90°	135°	
City centre											
Old City	2	0.54	15.6	4.6	10	0.52	0.30	0.34	0.29	0.33	0.16
Piasek Płd.	2_B	0.62	16.0	4.8	14	0.37	0.31	0.35	0.30	0.35	0.26
Kazimierz	2_B	0.68	12.7	4.1	12	0.40	0.22	0.24	0.22	0.25	0.26
Salwator	2_B	0.54	13.7	4.6	11	0.27	0.24	0.27	0.26	0.24	0.40
Residential											
Mistrzejowice 1	5_4	0.34	15.4	5.1	8	0.21	0.21	0.23	0.20	0.24	0.53
Mistrzejowice 2	5_4	0.29	12.3	4.0	13	0.17	0.17	0.13	0.12	0.19	0.63
Mistrzejowice 3	5_4	0.28	13.6	3.5	13	0.15	0.17	0.16	0.12	0.16	0.64
Mistrzejowice 4	5_4	0.79	13.8	4.8	11	0.17	0.18	0.17	0.13	0.20	0.54
Nowa Huta 1	5	2.54	12.7	3.4	16	0.19	0.16	0.17	0.15	0.17	0.58
Nowa Huta 2	5	0.69	13.1	3.3	16	0.21	0.18	0.19	0.18	0.18	0.55
Nowa Huta 3	5	0.54	12.8	3.1	17	0.19	0.17	0.18	0.15	0.18	0.58
Ugorek	5_4	0.24	12.5	6.5	14	0.19	0.20	0.22	0.17	0.18	0.61
Prądnik czerwony	5_4	0.38	13.8	7.3	10	0.17	0.18	0.19	0.14	0.18	0.64
Osiedle Europejskie	2	0.47	13.3	3.9	6	0.27	0.19	0.21	0.21	0.23	0.26
Bronowice 1	5_4	0.26	14.5	5.5	13	0.18	0.20	0.21	0.13	0.16	0.56
Kurdwanów	5	1.08	13.1	3.8	9	0.18	0.16	0.18	0.14	0.17	0.50
Ruczaj2	5	0.64	12.9	5.3	9	0.17	0.15	0.15	0.13	0.17	0.41
Single family housing											
Wola Justowska	6	0.79	6.8	2.4	10	0.19	0.11	0.11	0.11	0.11	0.70

Table 3 (continued)

Class	LCZ class	Area [km^2]	$H_{avb.}$ [m]	σ_b [m]	$H_{avt.}$ [m]	λ_{pb}	λ_{fb}				λ_{pv}
							0°	45°	90°	135°	
Osiedle Oficerskie	3_6	0.30	9.1	3.6	10	0.27	0.19	0.21	0.19	0.21	0.51
Pychowice	6	0.26	6.5	2.2	7	0.21	0.11	0.13	0.12	0.13	0.50
Tyniec	6	0.25	5.4	2.0	9	0.15	0.09	0.09	0.09	0.10	0.72
Ruczaj 1	6	0.34	6.3	2.6	9	0.23	0.14	0.16	0.13	0.15	0.50
Bronowice 2	6_9	0.26	6.9	2.0	8	0.17	0.09	0.11	0.10	0.11	0.72
Bronowice 3	6_9	0.21	6.1	2.1	8	0.16	0.09	0.09	0.09	0.10	0.73
Shopping centre											
CH Zakopianka	8	0.40	7.5	1.4	5	0.35	0.07	0.08	0.07	0.09	0.13
Galeria Bronowice	8	0.12	6.0	1.5	4	0.46	0.05	0.06	0.05	0.06	0.18
IKEA	8	0.14	7.2	1.3	1	0.29	0.05	0.06	0.06	0.07	0.14
CH Krokus	8_1	0.36	10.7	4.3	7	0.28	0.10	0.13	0.11	0.13	0.22
Galeria Kazimierz	2	0.06	12.5	3.3	5	0.50	0.16	0.20	0.17	0.20	0.13
M1	8	0.14	6.8	0.9	4	0.40	0.06	0.07	0.05	0.07	0.17
CH Bonarka	2	0.13	16.6	3.2	5	0.58	0.17	0.20	0.13	0.21	0.13
CH Plaza	8_5	0.04	15.3	2.5	6	0.46	0.11	0.11	0.12	0.15	0.18
Industrial											
ArcelorMittal	10	8.63	8.7	2.5	12	0.22	0.04	0.04	0.03	0.05	0.32
Skawina 2	10	0.38	9.9	3.3	6	0.20	0.10	0.08	0.08	0.11	0.44
Łęg	10	2.08	6.4	3.1	9	0.16	0.06	0.07	0.05	0.07	0.39
Rybitwy	10	2.63	5.5	1.5	7	0.21	0.05	0.06	0.05	0.07	0.32
Skawina 1	10	0.62	6.5	2.2	5	0.28	0.08	0.08	0.06	0.09	0.39
Urban greenery											
Park Jordana	B	0.23	6.1	1.1	19	–	–	–	–	–	0.82
Błonia	D	0.42	0.0	0.0	7	–	–	–	–	–	0.92

Table 3 (continued)

Class	LCZ class	Area [km^2]	$H_{avb.}$ [m]	σ_b [m]	$H_{avt.}$ [m]	λ_{pb}	λ_{fb}				λ_{pv}
							0°	45°	90°	135°	
Park Lotników	B_A	0.40	0.0	0.0	16	–	–	–	–	–	0.94
Zakrzówek	B	1.04	0.7	0.1	12	–	–	–	–	–	0.81
ROD Piast-Czyżyny	9	0.21	2.4	0.3	6	–	–	–	–	–	0.91

Appendix 2

See Table 4

Table 4 The morphometric characteristics of the surroundings of each measurement station (for determining the position of the station, see Fig. 2) obtained for squares of 0.81 km^2. The variables H_{avb}, H_{avt} and H_{av} are the average heights weighted by surfaces of buildings, trees and both, respectively, H_{max} is the maximum height of roughness elements, σ is the standard deviation of buildings and trees heights; λ_{pb}, λ_{pt} and λ_p^W are plan area indices for buildings, vegetation, and both of them in winter, respectively, λ_{f90} is the frontal area index for buildings calculated for wind sector $90^o \pm 22.5^o$

Station	LCZ[*1] Classes	λ_{pb}	λ_{pt}	λ_P^W	λ_{f90}	H_{avb} (m)	H_{avt} (m)	H_{av} (m)	H_{max} (m)	σ (m)	Terrain Max–Min (m)
R41	5_2	0.14	0.15	0.15	0.10	9.5	3.9	7.9	25.6	5.05	35.8
R42	6(West) A(East)	0.14	0.25	0.18	0.10	5.9	10.4	10.2	22.7	6.86	13.4
R43	3(South) C(North)	0.12	0.04	0.10	0.03	4.5	2.2	5.0	30.0	4.42	8.4
R45	6	0.15	0.07	0.15	0.07	6.3	5.4	5.9	25.0	3.78	4.6
R46	2_4(South) G_D (North)	0.24	0.10	0.23	0.17	9.7	5.9	9.2	23.5	4.70	10.7
R47	4_5	0.15	0.14	0.16	0.11	11.3	7.5	9.6	35.4	6.50	12.4
R48	4_5	0.07	0.15	0.10	0.08	7.0	6.2	7.9	35.0	7.58	25.9
R50	4	0.09	0.21	0.13	0.08	7.6	6.9	8.0	33.6	7.35	18.4
R51	6	0.09	0.16	0.11	0.06	5.1	4.0	4.7	19.5	3.89	35.9
R52	9	0.10	0.18	0.12	0.06	5.3	4.2	4.9	15.0	3.07	24.7
R53	6_5	0.14	0.29	0.19	0.13	8.6	9.7	8.6	35.0	5.43	10.0
R54	5_4	0.15	0.14	0.17	0.15	15.1	7.9	11.9	60.0	7.62	20.2
R56	4	0.18	0.17	0.20	0.13	13.1	6.6	11.1	55.0	6.94	30.8
R57	5_4	0.16	0.24	0.19	0.16	14.3	10.2	10.7	35.6	6.45	8.7
R58	5_4	0.20	0.17	0.22	0.13	12.7	7.8	11.2	55.0	6.84	22.7
R59	5_6	0.13	0.23	0.16	0.10	9.2	7.0	8.0	35.0	6.25	25.1
R60	5_9	0.13	0.25	0.20	0.13	8.6	6.3	6.7	30.0	4.51	11.1
R62	9	0.07	0.19	0.11	0.05	4.1	3.9	4.4	13.4	2.67	21.1
IMGW	6	0.11	0.24	0.15	0.09	6.2	5.6	5.6	15.0	2.63	31.9
AGH	4_A	0.20	0.24	0.25	0.19	11.8	10.5	11.6	40.0	6.21	12.2
UJ	2_A	0.26	0.20	0.26	0.17	10.8	9.2	11.0	25.0	5.59	14.7

References

Allwine KJ, Whiteman CD (1985) MELSAR: A mesoscale air quality model for complex terrain, vol 1—Overview. Technical description and user's guide. Pacific Northwest National Laboratory, Richland, Washington

Bajorek-Zydroń K, Wężyk P (eds) (2016) Atlas pokrycia terenu i przewietrzania Krakowa, MONIT-AIR. "Zintegrowany system monitorowania danych przestrzennych dla poprawy jakości powietrza w Krakowie", Kraków, ISBN: 978-83-918196-6-1 (in Polish)

Barlow JF, Dobre A, Smalley RJ, Arnold SJ, Tomlin AS, Belcher SE (2009) Referencing of street-level flows measured during the DAPPLE 2004 campaign. Atmos Environ 43:5536–5544

Bottema M (1995) Aerodynamic roughness parameters for homogenousbuilding groups—Part2: Results Document SUB-MESO 23. Ecole Centrale de Nantes, France

Britter RE (2005) DAPPLE: Dispersion of Air Pollutants and their Penetration into the Local Environment. http://www.dapple.org.uk
Britter RE, Hanna SR (2003) Flow and dispersion in urban areas. Annu Rev Fluid Mech 35:469–496
Burian SJ, Ching J (2009) Development of gridded fields of urban canopy parameters for advanced urban meteorological and air quality models. Environmental Protection Agency Technical Report EPA/600/R-10/007
Christen (2005) atmospheric turbulence and surface energy exchange in urban environments. Results from the basel urban boundary layer experiment (BUBBLE). Dissertation, Philosophisch-Naturwissenschaftlichen Fakultat der Universitat Basel, Basel, Switzerland
Cionco RM (1972) A wind profile index for canopy flow. Boundary-Layer Meteorol 3:255–263
Dobre A, Arnold SJ, Smalley RJ, Boddy JWD, Barlow JF, Tomlin AS, Belcher SE (2005) Flow field measurements in the proximity of an urban intersection in London, UK. Atmos Environ 39:4647–4657
Glotfelty T, Tewari M, Sampson K, Duda M, Chen F, Ching J (2013) NUDAPT 44 Documentation 04/25/2013
Grimmond CSB, Oke TR (1999) Aerodynamic properties of urban areas derived from analysis of surface form. J Appl Meteorol 38:1262–1292
Grimmond CSB, Salmond JA, Oke TR, Offerle B, Lemonsu A (2004) Flux and turbulence measurements at adensely built-up site in Marseille: Heat, mass (water and carbon dioxide), and momentum. J Geophys Res 109:D24101. https://doi.org/10.1029/2004JD004936
Gromke C, Buccolieri R, Di Sabatino S, Ruck B (2008) Dispersion study in a street canyon with tree planting by meansof wind tunnel and numerical investigations—evaluation of CFD data with experimental data. Atmos Environ 42:8640–8650
Hanna SR (2012) Urban boundary layer formulations for use in dispersion models. In: ICUC8—8th international conference on urban climates, 6-10.08.2012, Dublin, Ireland, paper no: 185
Hanna SR, Zhou Y (2009) Space and time variations in turbulence during the Manhattan Midtown 2005 field experiment. J Appl Meteorol Climatol 48:2295–2304
Hanna SR, White J, Zhou Y (2007) Observed wind, turbulence and dispersion in build-up downtown areas in Oklahoma City and Manhattan. Boundary-Layer Meteorol 125:441–468
Holland DE, Berglund JA, Spruce JP, MaKellip RD (2008) Derivation of effective aerodynamic surface roughness in urban areas from airborne lidar terrain data. J Appl Meteorol Climatol 47:26142626
Hussain M, Lee BE (1980) A wind tunnel study of the mean pressure forces acting on large groups of low-rise buildings. J Wind Eng Ind Aerodyn 6(1980):207–225
Kanda M, Inagaki A, Miyamoto T, Gryschka M, Raasch S (2013) A new aerodynamic parametrization for real urban surfaces. Boundary-Layer Meteorol 148:357–377
Kastner-Klein P, Fedorovich E, Rotach MW (2001) A wind tunnel study of organized and turbulent air motions in urban street canyons. J Wind Eng Ind Aerodyn 89:849–861
Kent CW, Grimmond CSB, Barlow J, Gatey D, Kotthaus S, Lindberg F, Halios CH (2017a) Evaluation of urban local-scale aerodynamic parameters: implications for the vertical profile of wind speed and for source areas. Boundary-Layer Meteorol 164:183–213
Kent CW, Grimmond CSB, Gatey D (2017b) Aerodynamic roughness parameters in cities: inclusion of vegetation. J Wind Eng Ind Aerodyn 169:168–176
Kent CW, Grimmond CSB, Gatey D, Barlow JF (2018a) Assessing methods to extrapolate the vertical wind-speed profile from surface observations in a city centre during strong winds. J Wind Eng Ind Aerodyn 173:100–111
Kent CW, Lee K, Ward HC, Hong JW, Hong J, Gatey D, Grimmond CSB (2018b) Aerodynamic roughness variation with vegetation: analysis in a suburban neighbourhood and a city park. Urban Ecosyst 21(2):227–243
Koizumi A, Motoyama J, Sawata K, Sasaki Y, Hirai T (2010) Evaluation of drag coefficients of poplar-tree crowns by a field test method. J Wood Sci 56:189. https://doi.org/10.1007/s10086-009-1091-8
Liao J, Wang T, Wang X, Xie M, Jiang Z, Huang X, Zhu J (2014) Impacts of different urban canopy schemes in WRF/Chem on regional climate and air quality in Yangtze River Delta, China. Atmos Res 145:226–243
Liu MK, Yocke MA (1980) Sitting of wind turbine generators in complex terrain. J Energy 4(1):10–16
Macdonald RW (2000) Modelling the mean velocity profile in the urban canopy layer. Boundary-Layer Meteorol 97:24–45
Macdonald RW, Hall DJ, Walker S (1998) Wind tunnel measurements of wind speed within simulated urban arrays, BRE Client Report CR 243/98, Building Research Establishment
Marht L (1982) Momentum balance of gravity flows. J Atmos Sci 39:2701–2711
Martilli A, Clappier A, Rotach MW (2002) An urban surface exchange parameterisation for mesoscale models. Bound-Layer Meteorol 104:261–304

Mayhead G (1973) Some drag coefficients for British forest trees derived from wind tunnel studies. Agric Meteorol 12:123–130

Mestayer PG, Durand P, Augustin P, Bastin S, Bonnefond J-M et al (2005) The urban boundary-layer field campaign in Marseille (UBL/CLU-ESCOMPTE): set-up and first results. Boundary-Layer Meteorol 114:315–365

PSU/NCAR (2005) Mesoscale modeling system tutorial class notes and users' guide (MM5 Modeling System Version 3). Mesoscale and Microscale Meteorology Division, National Center for Atmospheric Research (NCAR)

Raupach MR (1994) Simplified expressions for vegetation roughness length and zero-plane displacement as functions of canopy height and area index. Boundary-Layer Meteorol 71:211–216

Raupach MR (1995) Corrigenda. Boundary-Layer Meteorol 76:303–304

Rotach MW (1995) Profiles of turbulence statistics in and above an urban street Canyon. Atmos Environ 29:1473–1486

Rotach MW, Vogt R, Bernhofer C, Batchvarova E, Christen A, Clappier A, Feddersen B, Gryning SE, Martucci G, Mayer H, Mitev V, Oke TR, Parlow E, Richner H, Roth M, Roulet YA, Ruffieux D, Salmond J, Schatzmann M, Vogt J (2005) BUBBLE—an urban boundary layer meteorology project. Theor Appl Climatol. https://doi.org/10.1007/s00704-004-0117-9

Rudnicki M, Mitchell SJ, Novak MD (2004) Wind tunnel measurements of crown streamlining and drag relationships for three conifer species. Can J For Res 34:666–676

Schlunzen KH, Sokhi RS (eds) (2008) Overview of tools and methods for meteorological and air pollution mesoscale model evaluation and user training. Joint Report of COST Action 728 and GURME, GAW Report No. 181 WMO/TD-No. 1457

Scire JS, Robe FR, Fernau ME, Yamartino RJ (2000a) A user's guide for the CALMET Meteorological Model (Version 5.0). Earth Tech Inc., Concord

Scire JS, Strimaitis DG, Yamartino RJ (2000b) A user's guide for the CALPUFF Dispersion Model (Version 5.0). Earth Tech Inc., Concord

Stewart ID, Oke TR (2012) 'Local climate zones' for urban temperature studies. Bull Am Meteor Soc 93:1879–1900

Stewart ID, Oke TR, Krayenhoff ES (2014) Evaluation of the 'local climate zone' scheme using temperature observations and model simulations. Int J Climatol 34:1062–1080

Stull RB (1988) An introduction to Boundary Layer Meteorology. Kluwer Academic Publishers, Dordrecht

Sykes RI, Parker S, Henn D, Chowdhury B (2007) SCIPUFF Version 2.3Technical Documentation. L-3 Titan Corp, POB2229, Princeton, NJ 08543-2229

Tennekes H (1973) The logarithmic wind profile. J Atmos Sci 30:234–238

Tian J, Wang L, Li X, Gong H, Shi C, Zhong R, Liu X (2017) Comparison of UAV and WorldView-2 imagery for mapping leaf area index of mangrove forest. Int J Appl Earth Obs 61:22–31

Vollsinger S, Mitchell SJ, Byrne KE, Novak MD, Rudnicki M (2005) Wind tunnel measurements of crown streamlining and drag relationships for several hardwood species. Can J For Res 35:1238–1249

Xie M, Liao J, Wang T, Zhu K, Zhuang B, Han Y, Li M, Li S (2016a) Modeling of the anthropogenic heat flux and its effect on regional meteorology and air quality over the Yangtze River Delta region, China. Atmos Chem Phys 16:6071–6089. https://doi.org/10.5194/acp-16-6071-2016

Xie M, Zhu K, Wang T, Feng W, Gao D, Li M, Li S, Zhuang B, Han Y, Chen P, Liao J (2016b) Changes in regional meteorology induced by anthropogenic heat and their impacts on air quality in South China. Atmos Chem Phys 16:15011–15031